JOURNAL OF SPACECRAFT AND ROCKETS
Vol. 43, No. 4, July–August 2006

# Experiment of the Two-Dimensional Roughness Effect on Hypersonic Boundary-Layer Transition

Keisuke Fujii*
*Japan Aerospace Exploration Agency, Chofu, Tokyo, 182-8522, Japan*

DOI: 10.2514/1.17860

**An experimental investigation of the effects of two-dimensional roughness on hypersonic boundary layers was carried out at the JAXA 0.5 m hypersonic wind tunnel using a 5 deg half-angle sharp cone at a freestream Mach number of 7.1 and a wide range of stagnation conditions. Aerodynamic heating distributions and surface pressure fluctuations were measured with and without roughness elements applied to the cone. A wavy wall roughness with a wavelength of $2\delta$ located well upstream of the breakdown region had the effect of delaying transition. Surface pressure spectrum densities indicate that disturbances of the roughness wavelength are amplified compared to the smooth wall case. At a lower stagnation temperature, however, wavy wall roughness configurations had the same effect as regular roughness, and no discernible differences between wavy wall roughness and spherical roughness were observed, either in the transition point or in the pressure fluctuation spectrum.**

## Nomenclature

| | | |
|---|---|---|
| $C_p$ | = | pressure coefficient |
| $d$ | = | diameter of roughness spheres, m |
| $f$ | = | frequency, Hz |
| $k$ | = | roughness height, m |
| $M$ | = | Mach number |
| $P_{p\text{-}w}$ | = | Power spectrum density of surface pressure fluctuation, $\text{Pa}^2/\text{Hz}$ |
| $p$ | = | pressure, Pa |
| $p'$ | = | surface pressure fluctuation, Pa |
| $Re$ | = | Reynolds number based on boundary-layer edge values |
| $Re_k$ | = | roughness Reynolds number, $=\rho_k w_k k/\mu_k$ |
| $St$ | = | Stanton number evaluated at the boundary-layer edge condition and the adiabatic wall temperature of the laminar boundary layer |
| $T$ | = | temperature, K |
| $u$ | = | velocity, m/s |
| $x$ | = | streamwise distance from the cone apex, m |
| $\alpha$ | = | wave number, 1/m |

*Subscripts*

| | | |
|---|---|---|
| $e$ | = | value at the boundary-layer edge |
| $i$ | = | imaginary part |
| $o$ | = | stagnation condition |
| 2nd | = | value for the second mode instability |
| $k$ | = | value evaluated at the roughness height |

## I. Introduction

AMONG the factors affecting the transition of hypersonic boundary layers, the effect of surface roughness is of great importance from an engineering standpoint, for instance, when designing flight vehicles and testing using ground facilities. In fact, due to the current high demand for simulating in-flight flow conditions at higher Reynolds numbers than are achievable by conventional ground testing facilities, boundary-layer tripping methods have been studied and developed as essential wind tunnel testing techniques, especially with freestream speeds up to low supersonic. Extensive work by Braslow [1] has successfully established an engineering criterion for the minimum roughness height in terms of roughness Reynolds number, $Re_k$, to fix the boundary-layer transition point at or close to the tripping device. Braslow also mentioned that the effective roughness height increases quite rapidly with the edge Mach number when the Mach number exceeds approximately 4. In fact, tripping the hypersonic boundary layer sometimes requires the height of the roughness to be greater than the thickness of the boundary layer itself.

Recent investigations using hypersonic test facilities, including scramjet intake experiments at low angles of attack, have sometimes encountered difficulty in realizing sufficiently large Reynolds numbers. Ultimately it may be necessary to trip the boundary layer using roughness, while minimizing the height of the roughness to avoid undesirable effects on the flowfield. Several recent studies, including those of Berry et al. [2,3] have succeeded in finding efficient tripping configurations for inlet flow simulation that result in far fewer residual organized streamwise vortices in the tripped boundary layer than previous configurations. Their strategy is based on empirical knowledge that the creation of streamwise vorticity inside the boundary layer is very effective in causing transition. However, even with such efficient tripping configurations, the "effective" roughness is still higher than the boundary-layer thickness at a calculated edge Mach number of 4.4.

The hypersonic boundary-layer characteristic of lower sensitivity to surface roughness at Mach numbers greater than 4 reminded the author of the fact that the second mode starts to dominate in the linear instability mechanism from around that Mach number as well. Because it is widely known that noisy environments significantly affect boundary-layer transition [4], a question came to us as to whether certain configurations of roughness could affect the boundary layer as a noisy environment does. For instance, although the linear instability mechanism will not help to "fix" the transition at the roughness location as the bypass mechanism does, introducing disturbances of the second-mode frequency into the boundary layer could dramatically expedite transition even if the initial disturbance level were small, and this may be sufficient for some hypersonic testing purposes. Because the second mode is essentially a trapped acoustic wave inside the boundary layer, the boundary-layer's response to a two-dimensional wavy wall of a certain wave number which emits acoustic waves in a supersonic flow became the interest in the present study.

Since the author does not know of any other studies concerning the response of hypersonic boundary layers to the wavy wall roughness

Presented as Paper 0891 at the 43rd Aerospace Sciences Meeting and Exhibit, Reno, NV, 10–13 January 2005; received 26 May 2005; revision received 7 December 2005; accepted for publication 20 December 2005. 

*Researcher, Wind Tunnel Technology Center, 7-44-1 Jindaiji-Higashi, Chofu, Tokyo 182-8522, Japan, AIAA Member.

of the second-mode wavelength, the main objective of the present experiment is therefore to investigate that response and the evolution of disturbances induced by the roughness. Stanton number distribution and surface pressure fluctuation were measured for that purpose. The response of the boundary layer to a conventional sphere roughness configuration of the same height as the wavy wall roughness was also measured for reference purposes.

## II. Apparatus and Test

### A. Test Facility

This experiment was conducted using the Japan Aerospace Exploration Agency's 0.5 m hypersonic wind tunnel (JAXA HWT1), a pebble-heated blow-down facility with a nozzle exit diameter of 500 mm. Interchangeable axisymmetric contour nozzles provide uniform hypersonic flows at freestream Mach numbers of 5, 7, 9, and 11. The Mach 7 nozzle was selected for this experiment, to realize hypersonic flow over a wide range of stagnation conditions. Stagnation pressure could vary from 1 to 6 MPa and stagnation temperature could vary from 620 to 920 K, yielding freestream unit Reynolds numbers of $1.93 \times 10^6$ to $2.78 \times 10^7$/m. The freestream Mach number produced by the nozzle actually varies from 7.05 to 7.13 depending on the freestream unit Reynolds number. During the typical run time of about 20 s, it usually takes 8–12 s until the stagnation temperature becomes effectively constant. Measurements were therefore conducted 15 s after tunnel start. Detailed measurements of freestream turbulence or tunnel noise at this facility were not available at the time of the experiment; however, the results obtained from this experiment provided limited information on these as shown later.

### B. Model and Instrumentation

A sharp cone model of 5 deg half-angle shown in Fig. 1, was used to avoid the pressure gradient effect and the three-dimensional effect otherwise caused by side edges. The latter effect would exist with a flat plate model, because a relatively low stagnation pressure condition of the present test requires a rather long distance to the onset of transition compared with the nozzle exit diameter. The model is 800 mm overall in length and is composed of two parts: a tip section and a main body section. The 200 mm long tip section is made from tool steel to minimize surface contamination due to dust from the pebble heater located upstream of the nozzle throat. Three tip sections were fabricated: "tip C" with a two-dimensional wavy wall roughness of 2 mm interval and 0.5 mm height with a trapezoidal cross section; and "tip A" and "tip B" with smooth surfaces to which various types of roughness could be applied. The tip radii of tips A, B, and C were measured as 16, 9, and 15 $\mu$m, respectively, from micrographs taken before this series of tests. The rms surface roughness of the models were measured as 0.2–0.3 $\mu$m at the frustum and 0.4–0.5 $\mu$m at the tip sections. The step height of the tip-frustum junction was measured as 20–30 $\mu$m.

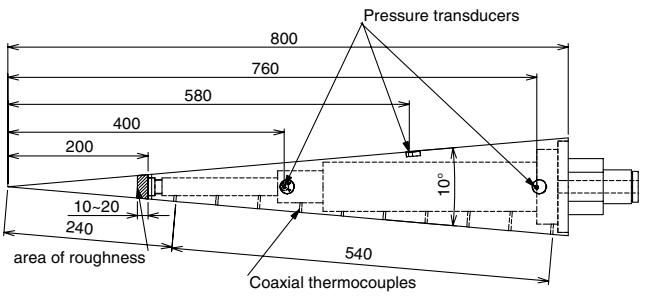


**Fig. 1 Schematic diagram of the cone model used in the experiment. Pressure transducers are located at $x = 400$, 580, and 760 mm from the apex. Three different tip sections are fabricated from tool steel to resist contamination due to particles in the stream. Coaxial thermocouples are installed over an area of $x = 240$–780 mm. Roughness elements are applied at the end of tip sections, at $x \approx 200$ mm.**

Transition was detected primarily by measuring heat transfer distributions using infrared (IR) thermography. To realize a large enough surface emissivity for infrared measurement, the model was painted black over half the cone, with the coating thickness measured at about 30–40 $\mu$m. The surface roughness of the coating was not measured, though it was polished as smooth as the model base surface before the tests. During the experiment, dust particles from the wind tunnel heater struck the coating, creating some roughness, but this did not have any observable influence on the transition. Ten coaxial thermocouples were installed under the black paint to complement the thermography. The main body section of the model was equipped with surface pressure transducers to measure surface pressure fluctuations at three locations to capture the influence of roughness on the disturbance evolution in the boundary layer. Because the estimated second-mode frequencies range as high as between 200 and 600 kHz, it was necessary for the transducers to have resonant frequencies higher than 1 MHz, as well as the ability to resolve small fluctuations in a very low-pressure environment as low as 400 Pa. A piezoelectric pressure transducer (PCB model 132A31) was selected as this has a resonant frequency above 1 MHz and a pressure resolution of 7 Pa. Three transducers were installed at $x = 400$, 580, and 760 mm from the cone apex. Because the transducers were flush with the cone surface, the transducer diameter of 1/8 in. practically limited the spatial resolution of fluctuation measurements. Because the second-mode wavelength at the sensor locations is roughly estimated to be between 3 to 10 mm depending on the stagnation condition, the pressure fluctuation data obtained here are expected to be quantitatively inaccurate, especially at high unit Reynolds numbers.

### C. Roughness Configurations

The two-dimensional wavy wall roughness in this experiment (Fig. 2a) had a wavelength of 2 mm and a height of 0.5 mm with a

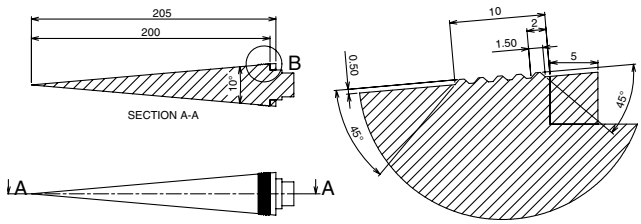


**(a) Wavy wall**

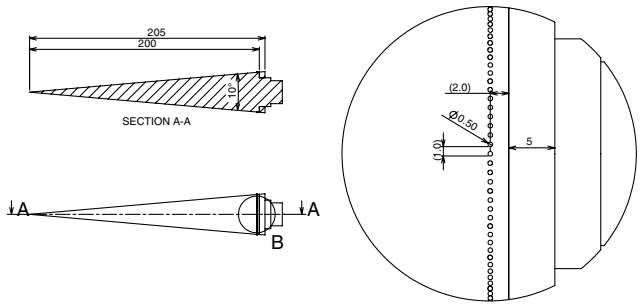


**b) Spheres**

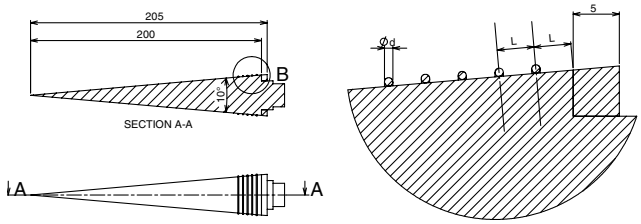


**c) Equally spaced wires $d$=0.45, 0.90 mm and $L$=2, 4 mm**

**Fig. 2 Detailed configuration of roughness elements, located at about 200 mm from the cone apex. All dimensions are in mm.**

**Table 1 Stagnation conditions and estimated values of the laminar boundary-layer thickness $\delta$ at the location of roughness ($x \approx 200$ mm)**

| | $T_o \approx 620$ K, $u_e = 1056$ m/s | | $T_o \approx 820$ K, $u_e = 1214$ m/s | | $T_o \approx 970$ K, $u_e = 1320$ m/s | |
|---|---|---|---|---|---|---|
| $p_o$, MPa | $\delta$, mm | $Re_{\text{unit}}$, 1/m | $\delta$, mm | $Re_{\text{unit}}$, 1/m | $\delta$, mm | $Re_{\text{unit}}$, 1/m |
| 1 | 2.4 | $4.9 \times 10^6$ | 2.5 | $3.1 \times 10^6$ | —— | |
| 2 | 1.7 | $9.7 \times 10^6$ | 1.8 | $6.2 \times 10^6$ | 1.8 | $4.8 \times 10^6$ |
| 2.5 | —— | | —— | | 1.6 | $6.0 \times 10^6$ |
| 4 | 1.2 | $2.0 \times 10^7$ | 1.3 | $1.3 \times 10^7$ | 1.3 | $9.6 \times 10^6$ |
| 6 | —— | | —— | | 1.1 | $1.4 \times 10^7$ |

**Table 2 Tested roughness parameters**

| Roughness configuration | Height mm | Location $x$, mm | Interval mm | Tip |
|---|---|---|---|---|
| Smooth | —— | —— | —— | Tip A |
| Spheres | 0.5 | 198 | —— | Tip B |
| Wavy wall | 0.5 | 198 | 2.0 | Tip C |
| Equally spaced wires (A) | 0.45 | 198 | 2.0 | Tip A |
| Equally spaced wires (B) | 0.45 | 195 | 4.0 | Tip A |
| Equally spaced wires (C) | 0.9 | 195 | 4.0 | Tip A |

trapezoidal cross section and was located $x = 188$–$198$ mm from the apex of the model. Estimated values of the boundary-layer thickness at $x = 200$ mm where the roughness was located are summarized in Table 1. Boundary-layer thickness was estimated from a velocity profile of a similar solution which was numerically calculated with the edge conditions of this experiment and assuming a surface temperature of 300 K. Because the surface temperature rise due to laminar aerodynamic heating during runs was 20 K or less, the assumption of a constant 300 K surface temperature seems reasonable. The boundary-layer edge condition calculated at a freestream Mach number of $M_\infty = 7.1$ is $M_e = 6.516$, $T_e/T_o = 0.1054$, and $p_e/p_o = 3.78 \times 10^{-4}$. Because of the effect of the relative wall cooling effect ($T_w/T_o$) on the boundary-layer profile, the decrease in unit Reynolds number due to the increase in stagnation temperature does not greatly affect the boundary-layer thickness estimation. This table suggests that the wavy wall roughness would introduce disturbances of "right" wavelength at stagnation pressure $p_o = 6$ MPa. Because the boundary-layer thickness is known to primarily determine the frequency of the second mode as $f_{2\text{nd}} \approx u_e/2\delta$ ([5]), the most unstable disturbance has a wavelength of approximately $2\delta$. Because the boundary layer grows downstream, however, the frequency and wave number of the largest amplitude decrease, and the roughness is only tuned to the second-mode wavelength at around the roughness location.

In addition to the two-dimensional wavy wall roughness, several other types of roughness element were also tested for reference. The roughness parameters and locations of the roughness examined in the present experiment are summarized in Table 2. A row of spheres configuration (Fig. 2b) was included since spheres have been applied in many previous experiments [6]. Spherical roughness elements were spot welded to a tip section at intervals of approximately $2d$, where $d$ is the sphere diameter. As an alternative to the wavy wall to introduce disturbances of the appropriate wavelength, a set of equally spaced wires (Fig. 2c) was also examined with an expectation that it would provide greater flexibility in generating different roughness heights and wavelengths while preserving the essential characteristics of the wavy wall roughness. These wires were firmly spot welded to the model at constant intervals that remained unchanged during the runs.

### D. Data Acquisition and Reduction

An aerodynamic heating rate was derived from the surface temperature trace measured by the infrared camera and coaxial thermocouples assuming the semi-infinite one-dimensional heat conduction, as is routinely employed in the facility [7]. However since the cone model is exposed to the flow from the tunnel start, the heating time becomes quite long, which could violate the simple assumption of infinite one dimensionality and so reduce the accuracy of the data. Lateral heat conduction effects are estimated by the ratio $\alpha(\partial^2 T/\partial x^2)/(\partial T/\partial t)$, which is expected to be approximately proportional to the error in the aerodynamic heating measurement ($\alpha$ here denotes thermal diffusivity). Because this ratio was lower than 5% in most cases in the experiment, it is believed that the obtained aerodynamic heating data are sufficiently accurate for the purpose of transition detection. Almost the entire painted region on the model, roughly $x = 210$–$760$ mm, was visible in the infrared thermographs.

Surface pressure data were sampled at 1 MHz starting at $t = 15$ s after tunnel start for a period of 66 ms. Dividing the data into 128 subsets, the power spectrum density was obtained by averaging each FFT result of the subsets.

## III. Results and Discussion

### A. Reference Data and Repeatability

To examine the effect of roughness on the transition location, a set of transition data were first obtained for a clean configuration without any roughness elements applied, and repeatability was examined. An IR image showing surface temperature distribution at $t \approx 20$ s from tunnel start ($t \approx 20$ s) under conditions of $p_o = 2$ MPa and $T_o \approx 820$ K is shown in Fig. 3 and indicates acceptable two dimensionality. Stanton number distributions along with a bottom line on the frustum at stagnation pressures of $p_o = 1$, 2, and 4 MPa with a stagnation temperature of $T_o \approx 800$ K are shown in the left column of Fig. 4. Although the lowest stagnation pressure case indicates no sign of transition on the model, the other two cases show a transition indicated by a gradual change of heat flux from laminar levels to turbulent levels. The beginning and the end of the transition are determined as indicated in the figures. The predictions of laminar and turbulent heat transfer, shown by dotted and dashed lines, respectively, are obtained by an engineering method developed by Zoby et al. [8].

Power spectra of surface pressure fluctuations obtained during the run of the corresponding figure in the left column are shown on the

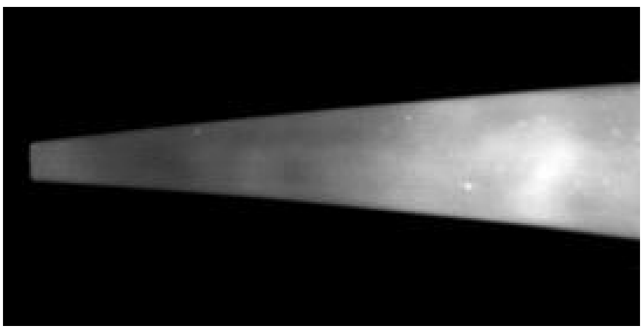

**Fig. 3 Infrared image from run 3854 showing surface temperature distribution at $t \approx 20$ s from tunnel start, where stagnation conditions are $p_o = 2$ MPa and $T_o = 820$ K. This confirms that acceptable two dimensionality is realized in these conditions. Flow direction is from left to right.**

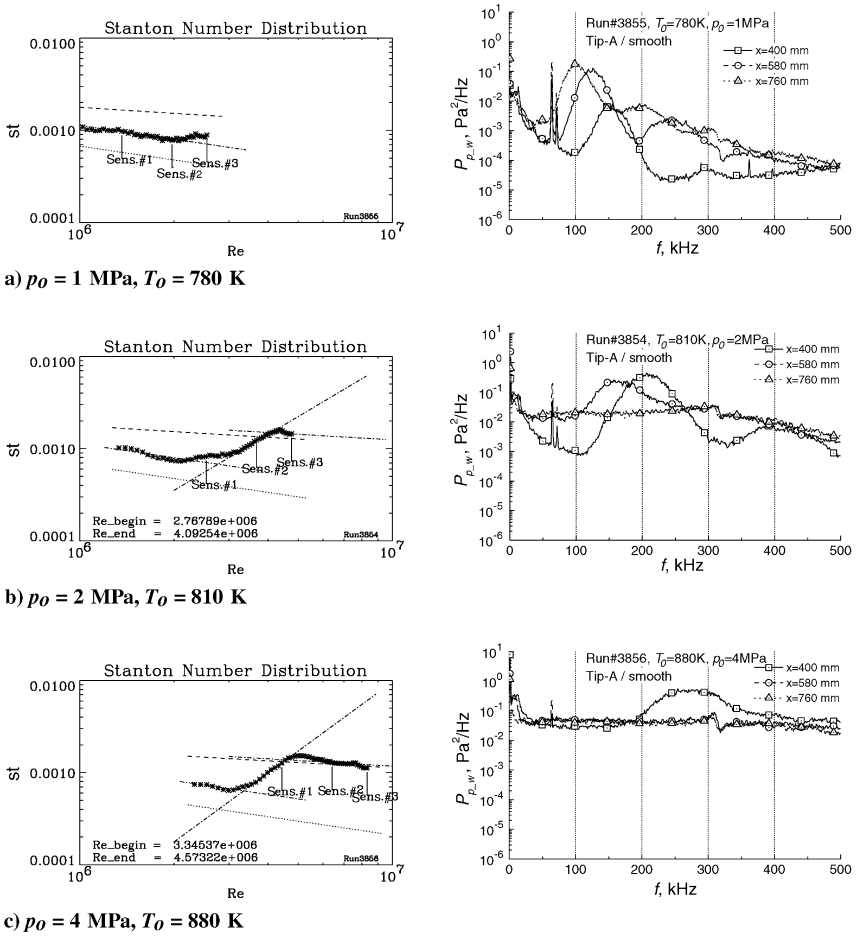


a) $p_0$ = 1 MPa, $T_0$ = 780 K

b) $p_0$ = 2 MPa, $T_0$ = 810 K

c) $p_0$ = 4 MPa, $T_0$ = 880 K

*St* versus $Re_x$ based on the distance from the apex  Power spectrum density diagram

**Fig. 4 Smooth wall test results of *St* distribution (left column) and power spectrum of surface pressure fluctuation (right column). The short vertical lines in the Stanton number figures indicate pressure transducer locations. Dotted and dashed lines in the left column figures, respectively, indicate predictions for the laminar and turbulent boundary layer.**

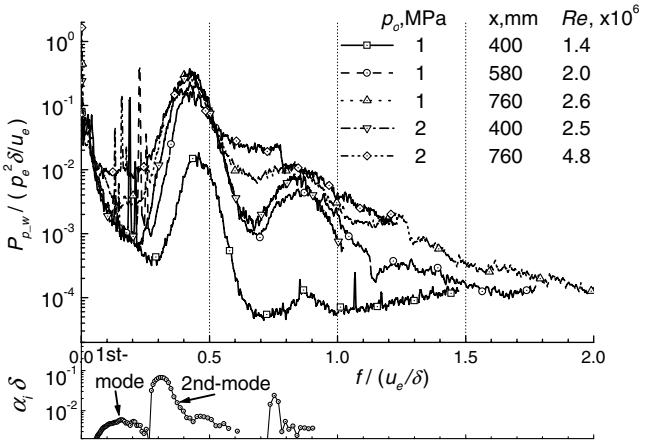


**Fig. 5 Nondimensionalized power spectrum densities versus nondimensional frequency (top) and nondimensional imaginary wave number calculated by an inviscid linear instability code (bottom). Frequencies of the large peaks in power spectrum densities collapse to approximately 0.5, indicating that these are second-mode disturbances.**

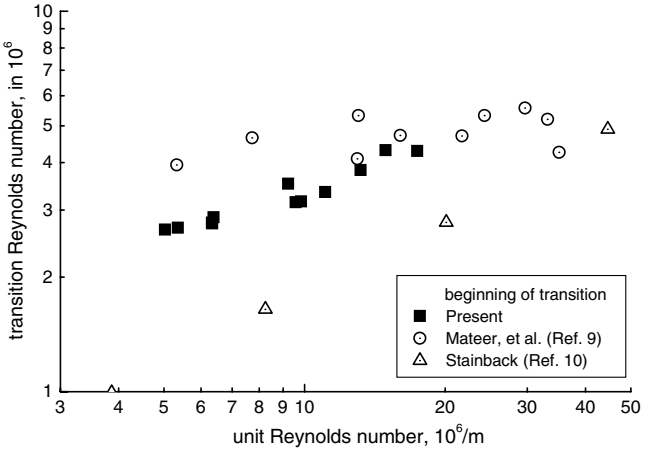


**Fig. 6 Transition Reynolds number versus unit Reynolds number obtained in the present experiment compared with data from other sources.**

right of Fig. 4. The second-mode amplification and subsequent breakdown to fully turbulent spectra can be clearly seen in the figures. In fact, when frequency is nondimensionalized with edge velocity and boundary-layer thickness (Fig. 5), all the peak frequencies are approximately a single value of 0.5, indicating that they correspond to the second-mode disturbances. Temporal inviscid linear stability analyses assuming a uniform wall temperature of 300 K and a similar boundary-layer profile are shown at the bottom of Fig. 5 and also indicate that the measured peak frequencies are related to the second mode. It should be noted here that the computed peak second-mode amplification rate is at a frequency lower than the measured peak amplitude by a factor of 0.72 in this case. This result reflects a downward shift in the frequency of the spectrum as the boundary layer thickens. It should be briefly

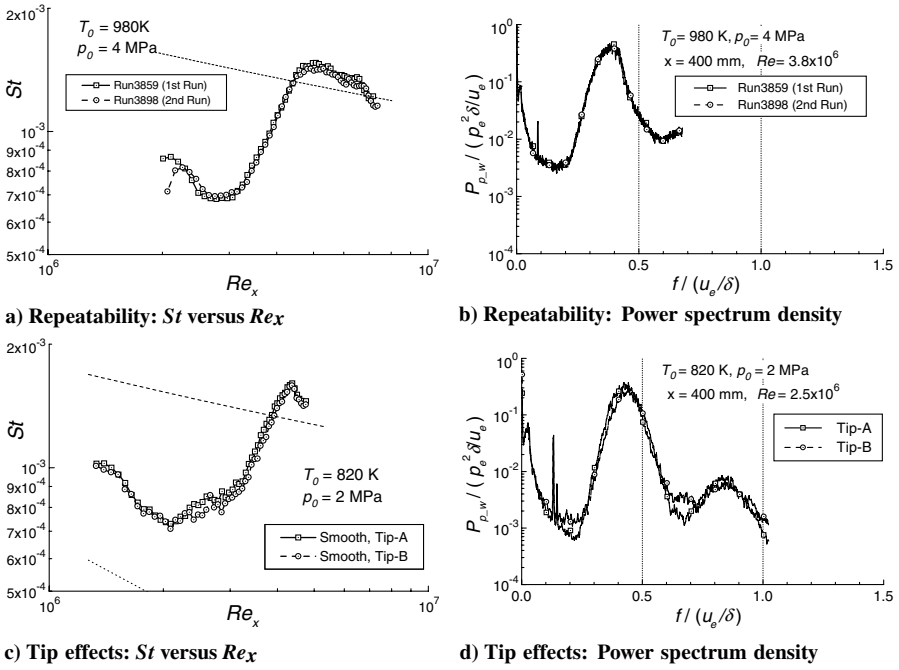


**a) Repeatability: *St* versus *Re*$_x$** **b) Repeatability: Power spectrum density**

**c) Tip effects: *St* versus *Re*$_x$** **d) Tip effects: Power spectrum density**

**Fig. 7 Results of repeatability a), b), and the effect of a different tip section on the transition c), d). Dashed and dotted lines in the *St* plot, respectively, indicate turbulent and laminar predictions [8].**

mentioned that the sharp spikes at $f \approx 60$ kHz in Fig. 4 are due to electrical noises as confirmed by results without flow, and the small leaps visible around $f \approx 300$ kHz are also believed to be due to electrical problems.

When the Reynolds number of the beginning of the transition is plotted versus the unit Reynolds number in Fig. 6, the result indicates a so-called unit Reynolds number effect, as observed in data from other conventional hypersonic facilities. Comparing with data obtained by Mateer and Larson [9] and Stainback [10], it is inferred that the present facility also has modest flow quality regarding freestream turbulence and noise. This dependence of the transition Reynolds number on the unit Reynolds number implies that tunnel noise affects the transition [11]; however, comparing data from different roughness configurations would be meaningful as long as the comparison were made under the same freestream conditions. Static pressure fluctuation in hypersonic wind tunnels is in general hard to measure due to the very low static pressure, and the author does not know of any static pressure fluctuation measurement data with sufficient frequency range. Although freestream noise or turbulence were not directly measured in this experiment, surface pressure fluctuation data can give limited information on these as long as the boundary-layer instability wave does not grow too large. The lowest unit Reynolds number condition in this experiment, which was at $T_o = 780$ K and $p_o = 1$ MPa (Fig. 4a) gives a fluctuation of the pressure coefficient at $x = 400$ mm of $C_{p,\mathrm{rms}} = 0.22\%$, $p'_{\mathrm{rms}}/p_e = 6.4\%$. It should be noted, however, that these values contain a linear instability wave to some extent and disturbances which resulted from the interaction between acoustic disturbances in the freestream and the boundary-layer receptivity mechanism.

Repeatability and the effects of slight changes in cone tip radius due to possible melting during high temperature and high pressure runs can be examined in Figs. 7a and 7b. Here, run 3859 was conducted at the beginning of this test series and run 3898 almost at the end. Both the Stanton number distributions and the power spectra of the pressure fluctuations at $x = 400$ mm are almost identical between these runs, showing excellent repeatability. The effect of the tip section between tip A and tip B is also examined at a stagnation temperature of 820 K and a stagnation pressure of 2 MPa. The Stanton number distributions shown in Fig. 7c are very close to each other. Similarly, the spectra of the pressure fluctuations (Fig. 7d) are essentially identical, with only minor differences.

### B. Wavy Wall Roughness Effect

*1. Cases of $T_o \approx 970$ K*

Figure 8 summarizes the results of the wavy wall roughness tests at stagnation conditions of $T_o \approx 970$ K and at $p_o = 2, 4$, and 6 MPa in terms of Stanton number versus Reynolds number. The figures show data for different roughness configurations: smooth surface (squares), wavy wall roughness (circles), and equally spaced wires (triangles). Three-dimensional sphere roughness of $\phi 0.5$ mm is overplotted as a widely used typical roughness geometry. All the results for $p_o = 2$ MPa form almost a single curve, indicating that all the roughness configurations are below the critical height in this condition. However, data for the two higher stagnation pressure conditions show that the wavy wall roughness has a weak but discernible effect in delaying transition compared with smooth wall data. The possibility that this may be due to a different tip from the smooth cases is eliminated when examining the curves labeled "tip-A wires" in Fig. 8b, which shows the case of five $\phi 0.45$ mm wires spot welded onto tip A at 2 mm intervals. This almost coincides with the wavy wall roughness (tip C) result. Because repeatability is remarkably good, as seen in Fig. 7a, it can be concluded that the delay in transition is a reflection of some physical phenomenon.

At $p_o = 6$ MPa (Fig. 8c) the wavy wall roughness (tip C) pushes the transition even further downstream. Although equally spaced wires are set at a 4 mm pitch in this case rather than 2 mm, both results of $\phi 0.45$ mm and $\phi 0.9$ mm show essentially the same effect.

According to a recent study on the receptivity of hypersonic boundary layers [12], receptivity to fast acoustic waves is greater than to slow waves. Because the wave number of a fast acoustic wave is lower than that of a slow wave of a particular frequency, the wave number of the wavy wall roughness would have a direct influence on the interaction between the roughness disturbance and the fast acoustic disturbance in the resonance condition with the eigenmodes. Figure 9 shows the neutral stability curve calculated by LSTAB, a linear stability code developed by the JAXA Supersonic Transport project unit [13], at a condition of $T_o = 1000$ K, $p_o = 6$ MPa, and $T_w = 300$ K. Throughout this series of experiments, the surface temperature rise at $x = 240$ mm due to laminar aerodynamic heating was 20 K or lower, and the effect of surface temperature change is assumed to be negligible at least at the roughness location of $x \approx 200$ mm. Because of the relatively strong wall cooling, the unstable region shown in the figure is due to the second-mode instability. Overplotting the wave number of the wavy wall

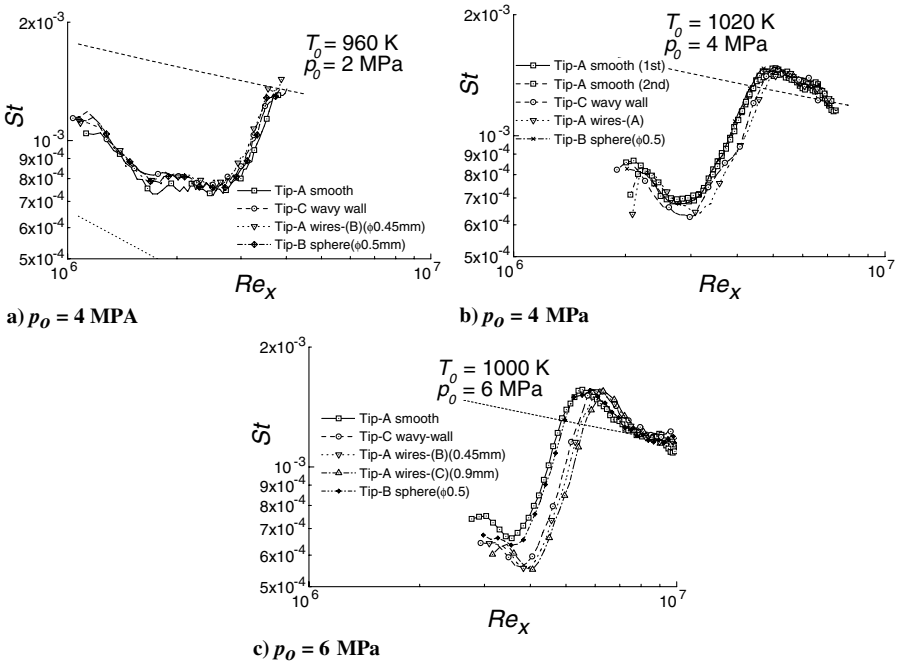


**Fig. 8 Comparison of wavy wall roughness results with smooth reference data at $T_o \approx 970$ K. Data for equally spaced wires and of $\phi 0.5$ mm spheres are overplotted. Dashed and dotted lines, respectively, indicate turbulent and laminar predictions [8].**

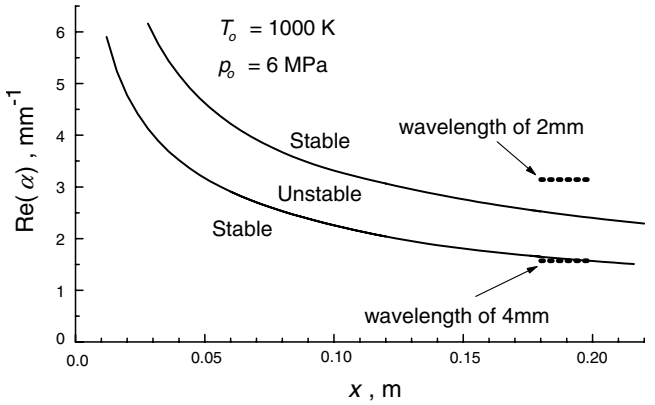


**Fig. 9 Neutral stability curve at $T_o = 1000$ K, $p_o = 6$ MPa, $M_e = 6.516$, and $T_w = 300$ K. Dashed lines indicate the roughness wave number and location.**

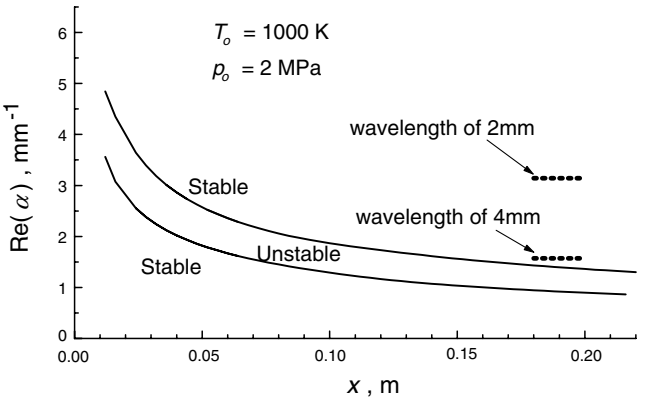


**Fig. 10 Neutral stability curve at $T_o = 1000$ K, $p_o = 2$ MPa, $M_e = 6.516$, and $T_w = 300$ K. Dashed lines indicate the roughness wave number and location.**

roughness of 2 mm wavelength and equally spaced wires of 4 mm pitch in the figure shows that the 4 mm pitch roughness is located at the lower edge of the neutral stability curve, whereas the 2 mm wavelength wavy wall roughness is beyond the unstable region. This is because the measured peak frequency (approximated roughly as $u_e/2\delta$) is higher than that of the peak second-mode amplification rate, as can be seen in Fig. 5. This relationship between the wave number of the roughness and that of the calculated peak second mode, especially for the 4 mm wavelength case, suggests that the interaction of the surface waviness and acoustic disturbances could indeed induce the second-mode disturbance, because a numerical example by Fedorov [12] shows that high receptivity is observed covering the instability region for fast acoustic waves with the adiabatic wall condition. The lower stagnation pressure case of $p_o = 2$ MPa, $T_o = 1000$ K, shown in Fig. 10, indicates that the thicker boundary layer results in a lower wave number of the unstable region. A major difference from Fig. 9 is that the roughness wave numbers are far beyond the calculated unstable region and that the subharmonics of the 4 mm wavelength are well below it. From these figures, it seems that the conditions in which the delay in transition was observed occur when the roughness wave number or its subharmonics are in the unstable second-mode region. It remains, however, uncertain as to how or whether such a relationship delays transition instead of expediting it.

When looking at how wavy wall roughness affects the boundary layer, only the pressure data of the lowest stagnation pressure case ($p_o = 2$ MPa) could give a clue, although no evident movement of the transition point can be observed for this condition, because for the other two conditions ($p_o = 4, 6$ MPa) the boundary layer seems to be in the process of breakdown at the locations of the pressure transducers. Figure 11a compares the power spectra of different roughness configurations at the stagnation condition. A difference from the smooth reference data is observed only within a limited frequency region, as illustrated in Fig. 11b. Because "tip-C wavy wall" has a 2 mm wavelength and "tip-A wires" ($\phi 0.45$ mm) have a 4 mm wavelength, the acoustic disturbances could be scattered to form fast acoustic mode waves at the roughness effectively with frequencies of 760 and 380 kHz, respectively, assuming $f \approx u_e + a/(\text{wavelength})$. The peak frequencies in Fig. 11b seem to roughly correspond to these frequencies or their subharmonics. From these results, it is possible that wavy wall roughness assists the propagation of fast acoustic waves of its wave number or subharmonics in the hypersonic boundary layer under the observed conditions. There still are many uncertainties regarding this

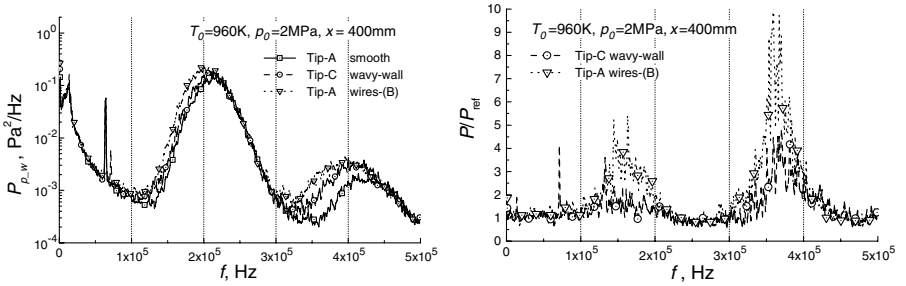


a) Power spectrum density b) Ratio of spectrum

**Fig. 11 Power spectrum densities of pressure fluctuations at $T_o \approx 960$ K, $p_o = 2$ MPa, and $x = 400$ mm. Data for roughness are compared with smooth surface data. $P_{\text{ref}}$ in b) denotes values of smooth wall data.**

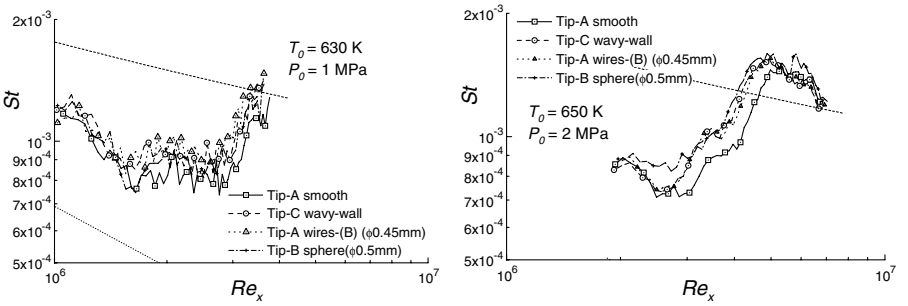


a) $p_O = 1$ MPa, $T_O = 630$ K b) $p_O = 2$ MPa, $T_O = 650$ K

**Fig. 12 Comparison of wavy wall roughness data with smooth reference data. Data for equally spaced wires ["wires (B)," see Table 2] and $\phi 0.5$ mm spheres are overplotted. Dashed and dotted lines, respectively, indicate turbulent and laminar predictions [8].**

hypothesis, since the eigenmodes of these frequencies themselves have only negative amplification rates from the roughness location to the sensor, whereas the observed differences are much larger than the preexisting disturbances. Considering again the excellent repeatability of the current test, however, the observed differences from the pressure spectrum of the smooth surface case are probably a reflection of physical phenomena.

### 2. *Cases of $T_o \approx 620$ K*

In contrast to the higher stagnation temperature cases, Fig. 12 shows that both the wavy wall roughness and the equally spaced wires resulted in an earlier transition than the smooth case. These results are actually almost identical to the case of spherical roughness of the same height. The pressure fluctuation data shown in Fig. 13 indicate a larger disturbance level than the smooth case over a wide range of frequencies. Again, the result for the wavy wall roughness is essentially the same as the result for the spherical roughness of the same height. This means that neither the wavy wall roughness nor the equally spaced wires excited a wave of a specific frequency, although the estimated second-mode frequencies for the conditions of Fig. 11a and 13 are not significantly different.

The calculated neutral stability curve for the lower stagnation temperature condition assuming a surface temperature of 300 K is shown in Fig. 14. Because relative wall cooling is weak compared with the higher stagnation temperature condition, the first-mode instability appears at $x \approx 120$ mm, which is earlier than the previous case. The relationship to the wave number is similar to the higher stagnation temperature cases, although the observed trend of the transition locations is quite different. It is worth noting that one difference from the higher stagnation temperature cases is that both the first and the second modes are active at the roughness location.

It must be mentioned here that it has been observed that a relatively large roughness size could delay the onset of transition. Holloway and Sterrett [14] reported that sphere-type roughness of fairly large height delays the transition of a boundary layer on a flat plate at a Mach number of 6, compared with cases without additional roughness. Because they did not acquire spectral information on fluctuating components, they only speculated that the laminar

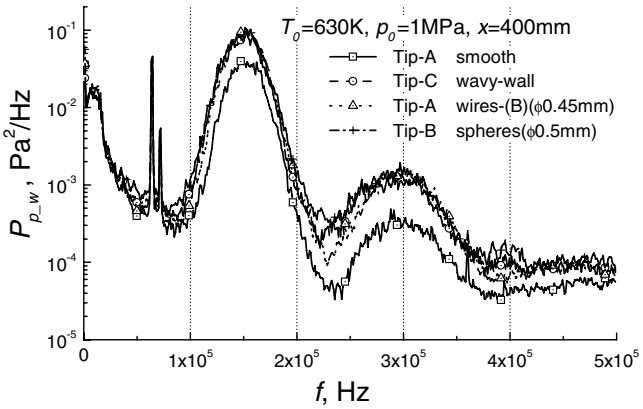


**Fig. 13 Power spectrum densities of pressure fluctuations at $T_o \approx 630$ K, $p_o = 1$ MPa, and $x = 400$ mm. Roughness data ["wavy wall" and "equally spaced wires (B)" in Table 2 and $\phi 0.5$ mm spheres] are compared with smooth wall data.**

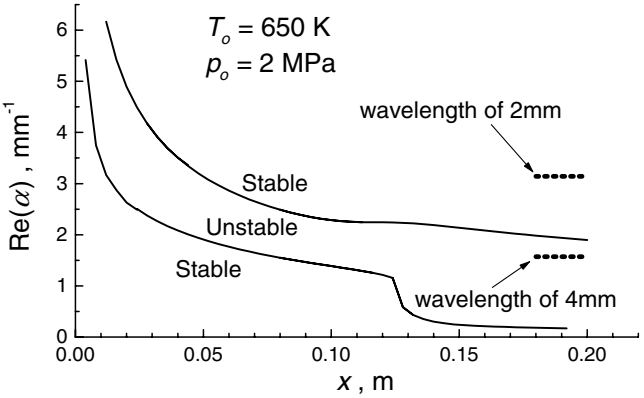


**Fig. 14 Neutral stability curve at $T_o = 650$ K, $p_o = 2$ MPa, $M_e = 6.516$ and $T_w = 300$ K. Dashed lines indicate the roughness wave number and location.**

separation that must exist near the small roughness elements could be at least partially responsible for the delay. Therefore, to determine the actual cause of the transition-delaying phenomenon observed in the present experiment, further experiments with even smaller roughness heights should be conducted so that additional disturbances can be rendered sufficiently small in the sense of perturbation theory. However, the pressure fluctuation spectral data presented in this paper provide new information about the response of the hypersonic boundary layer to two-dimensional periodic roughness.

## IV. Conclusion

An experimental investigation into tripping a hypersonic boundary layer to turbulence using two-dimensional wavy wall roughness was conducted at a Mach number of 7.1 and a wide range of stagnation conditions with a 5 deg half-angle sharp cone model at JAXA's 0.5 m hypersonic wind tunnel. Smooth wall results obtained as reference data provided freestream pressure fluctuation data along with natural transition data of the facility. These data suggest that the facility has modest flow quality regarding freestream turbulence and noise, and that the repeatability of both the transition location and the surface pressure fluctuation spectra are excellent.

A wavy wall roughness with a wavelength of $2\delta$ located well upstream of the breakdown region delayed the transition under some conditions. The observations obtained from the present experiment can be summarized as follows:

1) When the wavelength of the wavy wall roughness, or a quasiequivalent roughness composed of wires set at a regular pitch, is roughly equal to that of the unstable second-mode wavelength, a delay in the onset of the transition is observed for conditions of $T_o \approx 970$ K.

2) When the delay in transition is observed, the pressure fluctuations of certain frequencies increase compared to a smooth surface, and these frequencies correspond approximately to the roughness wave number if phase velocity is assumed to be $u_e + a$.

3) At low stagnation temperature ($T_o \approx 620$ K), wavy wall or quasiequivalent roughness configurations had the same effect as regular roughness, with no distinguishable difference either in the transition point or fluctuation spectra observed compared to spherical roughness.

Although it is possible that the observed delay in the onset of transition could be simply due to laminar separation behind the roughness, pressure fluctuation spectral data presented in this paper provide new information about the boundary-layer's response to two-dimensional periodic roughness.

## Acknowledgments

The present experiment would not have been accomplished without the great support of the Hypersonic Wind Tunnel Team, WINTEC, JAXA. The linear stability calculation was made with the assistance of the SST program unit, JAXA, especially Y. Ueda.

## References

[1] Braslow, A., Hicks, R., and Harris, R., Jr., "Use of Grit-type Boundary-Layer-Transition Trips on Wind-Tunnel Models," NASA, TR TN D-3579, 1966.

[2] Berry, S., Brauckmann, G., Bouslog, S., and Caram, J., "Shuttle Orbiter Experimental Boundary-Layer Transition Results with Isolated Roughness," *Journal of Spacecraft and Rockets*, Vol. 35, No. 3, 1998, pp. 241–248.

[3] Berry, S., Auslender, A., Dilley, A., and Calleja, J., "Hypersonic Boundary-Layer Trip Development for Hyper-X," *Journal of Spacecraft and Rockets*, Vol. 38, No. 6, 2001, pp. 853–864.

[4] Schneider, S., "Effects of High-Speed Tunnel Noise on Laminar-Turbulent Transition," *Journal of Spacecraft and Rockets*, Vol. 38, No. 3, 2001, pp. 323–333.

[5] Stetson, K., "Hypersonic Boundary-Layer Transition," *Advances in Hypersonics: Defining the Environment*, edited by J. Bertin, J. Periaux, and J. Ballmann, Vol. 1, Birkhäuser, Boston, 1992, pp. 324–417.

[6] van Driest, E., and Blumer, C., "Boundary-Layer Transition at Supersonic Speeds: Roughness Effects with Heat Transfer," *AIAA Journal*, Vol. 6, No. 4, 1968, pp. 603–607.

[7] Schultz, D., and Jones, T., "Heat Transfer Measurements in Short Duration Hypersonic Facilities," AGARD, TR AG-165, 1973.

[8] Zoby, E., Moss, J., and Sutton, K., "Approximate Convective-Heating Equations for Hypersonic Flows," *Journal of Spacecraft and Rockets*, Vol. 18, No. 1, 1981, pp. 64–70.

[9] Mateer, G., and Larson, H., "Unusual Boundary-Layer Transition Results on Cones in Hypersonic Flow," *AIAA Journal*, Vol. 7, No. 4, 1969, pp. 660–664.

[10] Stainback, P., "Some Effects of Roughness and Variable Entropy on Transition at a Mach Number of 8," AIAA Paper 67-132, 1967.

[11] Pate, S., and Schueler, C., "Radiated Aerodynamic Noise Effects on Boundary-Layer Transition in Supersonic and Hypersonic Wind Tunnels," *AIAA Journal*, Vol. 7, No. 3, 1969, pp. 450–457.

[12] Fedorov, A., "Receptivity of Hypersonic Boundary Layer to Acoustic Disturbances Scattered by Surface Roughness," AIAA Paper 2003-3731, 2003.

[13] Yoshida, K., Ogoshi, H., Ishida, Y., and Noguchi, M., "Numerical Study on Transition Prediction Method and Experimental Study on Effect of Supersonic Laminar Flow Control," NAL, TR SP-31, 1996.

[14] Holloway, P., and Sterrett, J., "Effect of Controlled Surface Roughness on Boundary-Layer Transition and Heat Transfer at Mach Numbers of 4.8 and 6.0," NASA, TR TN D-2054, 1964.

R. Kimmel
*Associate Editor*